

Article

Study of the Process of Electrochemical Oxidation of Active Pharmaceutical Substances on the Example of Nitrofurazone ((2E)-2-[(5-Nitro-2-furyl)methylene]hydrazine Carboxamide)

Vitalyi Vladimirovich Kuznetsov ^{1,2}, Natalya Andreevna Ivantsova ¹ , Evgenii Nikolaevich Kuzin ^{1,*} ,
Andrey Vladimirovich Pirogov ³, Yaroslav Olegovich Mezhuev ¹, Elena Alexeevna Filatova ¹
and Yulia Michailovna Averina ¹

¹ Mendeleev University of Chemical Technology of Russia, 125047 Moscow, Russia; vitkuzn1@mail.ru (V.V.K.); mezhuev.i.o@muctr.ru (Y.O.M.); filatova.e.a@muctr.ru (E.A.F.)

² Frumkin Institute of Physical Chemistry and Electrochemistry, 119071 Moscow, Russia

³ Lomonosov Moscow State University M. V., 119234 Moscow, Russia; pirogov@analyt.chem.msu.ru

* Correspondence: kuzin.e.n@muctr.ru

Abstract: The effective mineralization of nitrofurazone (10–100 mg L⁻¹) was performed in aqueous solutions in the presence of chloride ions by electrochemical treatment. The destruction of the organic pollutant molecules was due to their interaction with active oxygen- and chlorine-containing species forming at the inert anode (Pt/Ti or BDD) during electrolysis. Measurements of nitrofurazone concentration, chemical oxygen demand (COD) and total organic carbon (TOC) were used to estimate the removal efficiency of the pollutant. Both the pollutant oxidation rate and the degree of its mineralization were higher for the BDD anode due to the higher anode potentials on it in the course of electrolysis, which provides a high rate of active oxidizer species generation. As a result, practically full nitrofurazone molecule destruction (>99%) was achieved in 30 min at an anodic current density of 0.1 A cm⁻², a volume current density of 1.33 A L⁻¹ and pH 2 using BDD anodes. On the other hand, the nitrofurazone degradation efficiency was about 95% for Pt/Ti anodes under the same conditions. Additionally, byproducts of nitrofurazone electrooxidation were investigated by means of liquid chromatography-mass spectrometry (LC/MS). It was found that the initial decolorization of nitrofurazone solution, which occurs during the first 5 min of electrolysis, is due to the formation of a dichloro derivative of nitrofurazone, which causes the destruction of the π -conjugated bond system. Further electrolysis resulted in the almost complete destruction of the dichloro derivative within 30 min of electrochemical treatment.

Keywords: nitrofurazone; indirect electrochemical oxidation; mineralization; wastewater treatment



Citation: Kuznetsov, V.V.; Ivantsova, N.A.; Kuzin, E.N.; Pirogov, A.V.; Mezhuev, Y.O.; Filatova, E.A.; Averina, Y.M. Study of the Process of Electrochemical Oxidation of Active Pharmaceutical Substances on the Example of Nitrofurazone ((2E)-2-[(5-Nitro-2-furyl)methylene]hydrazine Carboxamide). *Water* **2023**, *15*, 3370. <https://doi.org/10.3390/w15193370>

Academic Editors: Ying Zhang and Fangke Yu

Received: 14 August 2023

Revised: 15 September 2023

Accepted: 21 September 2023

Published: 26 September 2023



Copyright: © 2023 by the authors. Licensee MDPI, Basel, Switzerland. This article is an open access article distributed under the terms and conditions of the Creative Commons Attribution (CC BY) license (<https://creativecommons.org/licenses/by/4.0/>).

1. Introduction

The degradation of surface waters is one of the key issues of the modern world, and it has attracted attention worldwide. Population growth, an increase in industrial production, as well as the development and implementation of new materials and technologies have led to the complicated composition of wastewater. As a result, current wastewater treatment methods are ineffective. For this reason, the development of innovative, highly effective methods of wastewater treatment is relevant. Specific pollutants, the neutralization of which is undoubtedly necessary, are active pharmaceutical ingredients (APIs). Increasing the use of antibiotics in agriculture results in a significant increase in API emissions into the environment and, in particular, in the hydrosphere [1–3]. The bioaccumulation of APIs, the inhibition of vital activities of microorganisms, the formation of resistant and highly toxic complexes, biocenoses degradation and the emergence of resistant strains of microorganisms should be mentioned among the negative consequences of the entry of APIs into the environment [4–7]. The contamination of domestic wastewater by APIs

is another consequence of their use, which can lead to the complete inactivation of deep biological wastewater treatment and, therefore, the discharge of wastewater with a high content of nutrients into various water bodies, which causes eutrophication. According to various sources, antibiotics and their metabolites are already found in both natural [8,9] and domestic wastewater [10]. Solving this problem is urgent, not only for countries with significant sources of fresh water [11], but also for countries that produce drinking water through the desalination of sea or ocean water [12–18]. Antibiotics and their metabolites are just the tip of the iceberg. The chemical contamination of wastewater by other forms of APIs is, essentially, not controlled. Nonsteroidal anti-inflammatory drugs, hormonal drugs (contraceptives), antihistamines, antibacterials (with the exception of antibiotics), antivirals and painkillers, unlike antibiotics, are not subject to strict control in many countries. For this reason, they are used far more often. Their entry into the environment can exceed the volumes of antibiotics entry by an order of magnitude [19,20]. Since the health effects of these pollutants have not yet been fully studied, they can be hazardous for both humans and nature.

Many studies devoted to the issues of the purification of both natural waters and wastewater from various kinds of pharmaceutical substances have been recently published [21–26]. They describe the treatment of model or real wastewater containing less than 1 mg L^{-1} APIs. Advanced oxidation processes (AOPs) are traditionally used for the destruction of API molecules. The combination of catalytic photo-oxidation processes and oxidation with Fenton's reagent and ozone makes it possible to destruct microamounts of APIs with high efficiency and the formation of a minimal amount of organic metabolites. The high efficiency of AOPs is due to the formation of highly active oxidizers, namely, the hydroxyl radical, hydroperoxyl radical, ozone and other species, which are significantly superior in their oxidative power to most individual oxidative agents. Data on the redox potentials of some oxidizers generated in AOPs are given in Table 1 [27–29].

Table 1. Standard oxidation potentials of some oxidizers in aqueous solutions.

Oxidant	OH•	O ₃	H ₂ O ₂	Hydroperoxyl Radicals	Cl ₂	O ₂
Standard oxidation potential $E^{\circ}_{298.15}/\text{V vs. SHE}$	2.80	2.07	1.77	~1.70	1.36	1.23

Despite all of the advantages described above, the use of AOPs is only reasonable for trace amounts of APIs in waste or natural waters. The treatment of more concentrated wastewater ($c(\text{APIs}) > 10 \text{ mg L}^{-1}$) becomes either insufficiently effective or too expensive [30,31]. The use of supercritical water oxidation (SCWO) is relevant in these cases. Although SCWO has demonstrated high efficiency in wastewater purification, its application requires high energy consumption and only becomes economically feasible if there is a significant amount of organic compounds in the treated water, which are a source of thermal energy for the process.

Untreated pharmaceutical industry wastewater contains relatively high ($>5 \text{ mg L}^{-1}$) concentrations of nitrofurazone. The use of AOPs associated with treatment with ozone or Fenton's reagent is not effective in this case, since it will lead to a large consumption of the reagents. In addition, the turbidity of real wastewater can be rather high, which makes photochemical methods inefficient. Electrooxidation is one of the methods for AOPs, which can be used alone or in combination with other methods for wastewater treatment. It is suitable for the local purification of industrial wastewater containing high concentrations of APIs. Electrooxidation can provide a high degree of mineralization of pollutants, while the residue amounts can be further oxidized using advanced oxidative processes [32–35]. Electrochemical treatment has recently been successfully applied to the degradation of paracetamol [36] and tetracycline [37] in aqueous solutions. The efficiency of electrooxidation for the decomposition of such difficult-to-oxidize compounds, such as non-ionic surfactants based on ethers, was shown in [38]. The mechanism of electrooxidation

is mainly divided into direct and indirect mechanisms [39]. Direct oxidation means that the organic molecule is oxidized on the anode by direct electron transfer. The processes of direct oxidation are very important in electroorganic synthesis; however, their role in electrodestruction is limited. Indirect oxidation implies the generation of active species at the anode (Table 1), which further react with pollutant molecules. The full mineralization of organic molecules during the processes of indirect oxidation may be due to the high oxidation power of species generated during electrolysis.

Nitrofurazone ((2*E*)-2-[(5-Nitro-2-furyl)methylene]hydrazine carboxamide) (Figure 1) is antibiologically active against both Gram-positive and Gram-negative bacteria. Its chemical formula is given below:

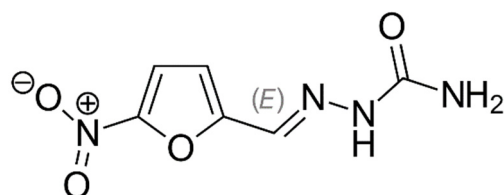


Figure 1. Chemical formula of nitrofurazone.

The use of nitrofurazone in the treatment of animal diseases, in particular, in animal husbandry, is still widespread. Moreover, it is still very popular as a topical solution for the treatment of tonsillitis in Russia and some other countries. Therefore, the neutralization of wastewater containing nitrofurazone is an urgent task, which should be solved in the near future taking into account environmental management requirements [40–42]. Since synthetic pollutants are not removed by conventional wastewater treatment plants, the costs of neutralizing them can be high [40]. The rational choice of electrode material and electrolysis conditions is needed for cost reduction [41]. In this study, nitrofurazone was chosen as a model active pharmaceutical substance to evaluate the possibilities and limitations of electrochemical methods for the destruction of small API molecules. Nitrofurazone is a heterocyclic compound containing electron-withdrawing groups, which hinders its oxidation. It should be noted that data on the indirect electrochemical oxidation of nitrofurazone, the degree of its mineralization, as well as the products of its electrochemical transformations, are lacking in the literature. A quite complex photoelectrochemical method for nitrofurazone removal was proposed in [43], in which about 80% of pollutant removal was achieved within 10 h.

Electrochemical treatment methods can be applied for the mineralization of nitrofurazone [44]; however, a number of issues need to be solved before using them. Firstly, the electrochemical oxidation of organic pollutants of complex chemical nature can be incomplete, which results in the accumulation of various metabolites in aqueous solutions under the treatment. The incomplete oxidation products can be highly toxic, and their accumulation in wastewater is completely unacceptable. Therefore, the identification of metabolites is necessary for the evaluation of the possibility of using electrochemical methods. Secondly, it is necessary to determine the time for wastewater treatment, as well as to choose the optimal solution composition and electrolysis conditions. Based on the above, the aims of the present study were: (1) to estimate the efficiency of the use of electrochemical oxidation for wastewater containing relatively high concentrations (10–100 mg L⁻¹) of nitrofurazone; (2) to find a degree of organic pollutant mineralization in the course of electrochemical treatment; (3) to identify metabolites of nitrofurazone electrooxidation and, therefore, to estimate the safety of electrochemical methods for wastewater treatment.

2. Material and Reagents

Aqueous solutions containing 10–100 mg L⁻¹ nitrofurazone were used for electrooxidation. To prepare them, the required amount of Avexima© (Russian Federation), a drug based on nitrofurazone, was dissolved in distilled water. According to the manufacturer, one pill contains 20 mg nitrofurazone, 100 mg sodium chloride and excipients: tartaric

acid, sodium bicarbonate, sodium carbonate, macrogol and medium molecular weight povidone. The drug was crushed and ground in an agate mortar. After that, the necessary amount of the powder (in terms of nitrofurazone) was weighed using an analytical balance (CAS CAUW-120D, South Korea) and dissolved in 0.75 L of deionized water. The solution was stirred using a magnetic stirrer with slight heating of the solution ($t \approx 50\text{ }^{\circ}\text{C}$). After that, the solution was filtered from insoluble impurities using the Büchner funnel with the Millipore membrane ($0.45\text{ }\mu\text{m}$ pore size, 47 mm diameter). The resulting solution was transparent. The concentration of nitrofurazone in the prepared solutions was determined by its specific reaction with a 10 wt.% solution of decarbonized sodium hydroxide resulting in the appearance of an orange color. The optical density of solutions ($\lambda = 450\text{ nm}$) was measured on a photoelectric colorimeter DR 2800 (HACH, Ames, IA, USA).

The concentration of chloride ions in solutions under electrochemical treatment varied within 0.001–0.010 M, which was five times higher than the concentration of nitrofurazone and corresponded to the level of chloride ions in natural waters. The oxidation of chloride ions on the inert anode, followed by the interaction of oxidation products with water molecules, leads to the formation of highly-active chlorine-containing species, e.g., HClO, OCl^{\bullet} in the solution under electrochemical treatment. Since an activation barrier of redox reactions involving them is low, this facilitates the destruction of organic pollutant molecules. However, the interaction of chlorine-containing species with organic molecules can lead to the formation of toxic chlorine derivatives. Therefore, it is necessary to control their formation and avoid their accumulation in treated aqueous solutions.

Preliminary experiments on the electrochemical oxidation of nitrofurazone were carried out in cells with both separated and undivided cathode and anode compartments. As was later shown, the effective oxidation of nitrofurazone is only possible in cells with separated spaces (see below); it occurs in the anolyte. A cation exchange membrane (Nafion[®]) was used (Figure 2) in the experiments on nitrofurazone electrooxidation. It allows for stabilizing the acidity of the anolyte. Since the hydronium ions transfer number is large enough, H^+ -ions form during electrolysis at the anode transfer through the membrane without causing excessive acidification of the solution in the anode compartment of the electrochemical cell.

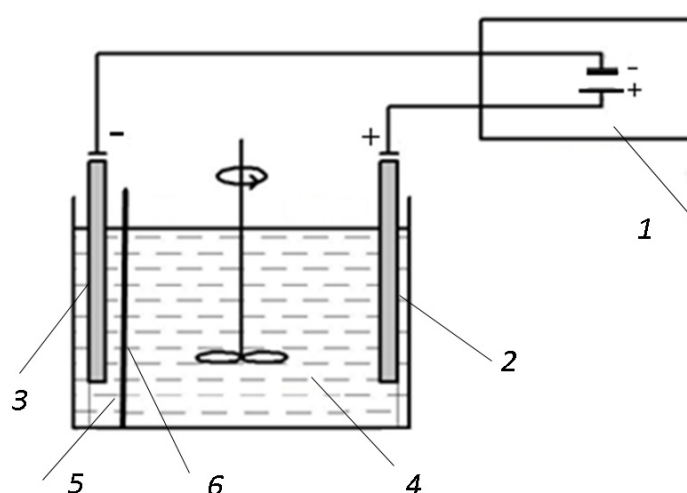


Figure 2. Electrochemical reactor. 1-DC source, 2-anode, 3-cathode, 4-anodic compartment ($V = 150\text{ mL}$), 5-cathodic compartment ($V = 50\text{ mL}$), 6-cation exchange membrane.

The volume of the anolyte was 150 mL. Sulfuric acid was added to the solution under electrochemical treatment in such a way that its concentration was $\sim 0.01\text{ M}$ in order to increase its electrical conductivity and facilitate the oxidation of the organic pollutant. The cathodic compartment of the electrolyzer ($V = 50\text{ mL}$) was filled with $0.01\text{ M H}_2\text{SO}_4$ ($\text{pH} \approx 2.0$).

The electrooxidation of nitrofurazone was carried out on platinized titanium or boron-doped diamond (BDD) anodes with $S_{\text{geom}} = 2 \text{ cm}^2$. A counter electrode was a mesh of platinized titanium. Electrolysis was performed in galvanostatic mode using a DC source DAZHENG PS-305D (China). The solution was stirred with a magnetic stirrer. In the course of the preliminary experiments, it was found that the rapid decoloration of the solution under electrochemical treatment, and, hence, the oxidation of nitrofurazone, occurs when the current passing through the cell is more than 0.15 A. For this reason, $I = 0.2 \text{ A}$ was chosen for the electrochemical destruction of a pollutant. This value corresponds to the anodic current density of 0.1 A cm^{-2} and the volume current density per the volume of the anolyte of 1.33 A L^{-1} .

The efficiency of the nitrofurazone removal was calculated using the formula:

$$\text{Removal efficiency (\%)} = \frac{C_0 - C_i}{C_0} \cdot 100\%,$$

where C_0 (g L^{-1}) is the initial concentration of the pollutant, C_i (g L^{-1}) is the concentration of the pollutant after electrochemical treatment.

The rate of pollutant degradation can be expressed by the formula [42]:

$$-\frac{dC}{dt} = k \cdot C^\alpha \cdot C(\text{Ox})^\beta,$$

where C (g L^{-1}) is the concentration of the pollutant, t (min) is the treatment time, k is the Arrhenius constant in the relevant units, $C(\text{Ox})$ (mol L^{-1}) is the concentration of active oxidizing species in the solution, which is approximately constant in steady state electrolysis. Under conditions of constant $C(\text{Ox})$, one can write:

$$-\frac{dC}{dt} = k' \cdot C^\alpha$$

If the reaction obeys a first order equation ($\alpha = 1$):

$$-\frac{dC}{dt} = k' \cdot C, \text{ and}$$

$$C = C_0 \cdot e^{-k't}$$

where k' is the rate constant (min^{-1}). Therefore, the dependence of $\ln C$ vs. t is a straight line in the case of the first-order equation, which makes it possible to determine the rate constant.

A digital potentiostat IPC-Pro MF (Volta, Russian Federation) was used for voltammetric measurements. The potential of the working electrode was set and measured versus the Ag/AgCl reference electrode in saturated KCl solution. In the present paper, all electrode potentials are given against this electrode unless otherwise stated. The processing of experimental data was performed using Origin 8[®] software (Cheshire, CT, USA).

To estimate the degree of organic pollutant destruction, the chemical oxygen demand (COD), total organic carbon content (TOC) and the open-circuit potential of Pt/Pt electrode (ORP) were measured. In addition, since formaldehyde and monobasic carboxylic acids can potentially be formed during electrooxidation, it is also necessary to determine their concentrations in the solution under electrochemical treatment. The color reaction with phenylhydrazine and potassium ferricyanide in an alkaline medium was used for the determination of formaldehyde, and the reaction with ammonium metavanadate was used for carboxylic acid detection.

The identification of organic metabolites that can potentially accumulate in aqueous solutions of nitrofurazone in the course of electrochemical treatment was performed using the HPLC-MS technique. The analysis was carried out on a hybrid mass-spectrometer for tandem mass spectrometry QTrap 3200 AB Sciex (Canada). The device was equipped

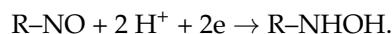
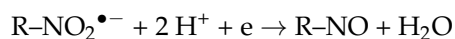
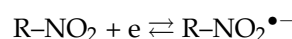
with two ion sources: Turbo Spraytm (electrospray ionization) and Heated Nebulizertm (chemical ionization at atmospheric pressure). The separation of organic substances was performed using Acclaim RSLC. The sample was loaded in solvent A (0.5% aqueous solution of formic acid) followed by gradient elution with solvent B (acetonitrile) over 39 min according to the following program: 0.00–2 min—20% B, 2–31 min—20–100% B, 31–35 min—100% B, 35.1–39 min—20% B. A full survey mass scan was performed in the interval of an m/z range of 50–1070.

The use of the HPLC-MS technique was due to the complex chemical nature of the mixtures of species formed during electrolysis. Intermediates formed in the course of electrochemical treatment have similar chemical structures, and it is necessary to separate them before, for instance, NMR analysis. This was beyond the scope of this study.

3. Results and Discussion

3.1. Electrochemical Behavior of Nitrofurazone

According to the literature data, nitrofurazone is electrochemically active in aqueous solutions [45,46] due to easily reduced nitro groups in its molecule. Nitrofurazone reduction waves were used for its quantitative determination by means of electrochemical sensors [46]. The mechanism of nitrofurazone electroreduction is quite complex, includes several electrochemical stages and finally leads to the formation of a hydroxylamine (RN-HOH) derivative. The route of nitrofurazone electrochemical reduction depends on both the electrode material and the pH of the solution, and can generally be represented as follows [46]:



Nitro radicals forming at the first stage of nitrofurazone electroreduction react with oxygen molecules under aerobic conditions, resulting in the formation of suboxide radicals, which can later be transformed into hydrogen peroxide. It is very likely that the antimicrobial activity of nitrofurazone solutions is due to these reactions.

Voltammetric measurements showed two reduction waves of nitrofurazone in acidic solution at the Pt/Ti electrode (Figure 3). The redox transitions are irreversible because both the electrode potentials and the electrical charges corresponding to them depend on the scan rate.

There were no responses associated with the electrochemical transformation of nitrofurazone in the anodic region of potentials. The destruction of nitrofurazone molecules at high anodic potentials is due to their interaction with highly reactive oxygen- ($\text{O}_2^{\bullet-}$, $\text{HO}_2^{\bullet-}$, etc.) or chlorine- (ClO^{\bullet} , HClO) containing species generated at the anode [47]. From a practical point of view, anodic oxidation is preferable for wastewater treatment since it can lead to the complete destruction of organic molecules, which avoids the accumulation of toxic metabolites in wastewater. The cathodic and anodic compartments of the electrochemical cell should be separated to prevent the useless consumption of the electrical charge in the reduction of nitrofurazone at the cathode and the subsequent oxidation-formed products at the anode. In addition, the interaction between reactive intermediates of the cathode and anode reaction results in the formation of unpredictable products during the electrochemical treatment, the potential danger of which is unknown. The separation of the cathode and anode compartments of the electrolytic cell avoids the mixing of cathodic and anodic reaction products.

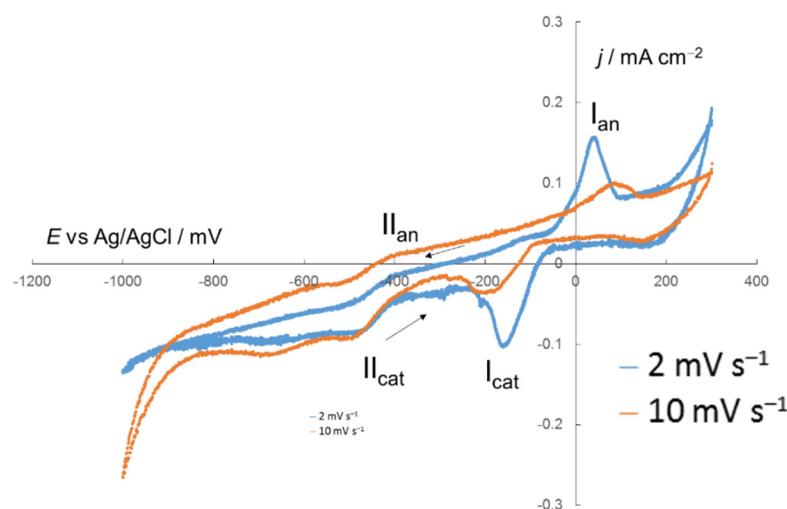


Figure 3. Cyclic voltammograms in solution of nitrofurazone (26.7 mg L^{-1}) obtained by dissolving Avexima[®] in $0.01 \text{ M H}_2\text{SO}_4$. Numbers I and II correspond to the redox transitions of nitrofurazone in the cathodic region of potentials (cat—redox transitions on the cathodic scans of CVs, an—redox transitions on the anodic scans of CVs). See comments in the text.

The use of a cation-exchange membrane prevents the acidification of analytes due to the transport of hydronium ions formed during water molecule oxidation through them toward the cathode. The solution containing nitrofurazone should be placed into the anodic compartment of the electrolyzer (see above). All subsequent experiments were performed under such conditions.

3.2. Electrooxidation of Nitrofurazone

According to the optical density of solutions measurements ($\lambda = 450 \text{ nm}$), nitrofurazone is effectively oxidized at a platinized titanium anode (Figure 4a). Decoloration of the solution occurs in the first 10 min of electrolysis. The color of nitrofurazone is due to the $\pi\text{-}\pi^*$ electron transition in the π -conjugated system of the molecule. Electrooxidation leads to the destruction of the system of π -conjugated bonds, which results in the disappearance of the absorption maximum at 320–400 nm in the UV-Visible spectrum (Supplementary Figure S1).

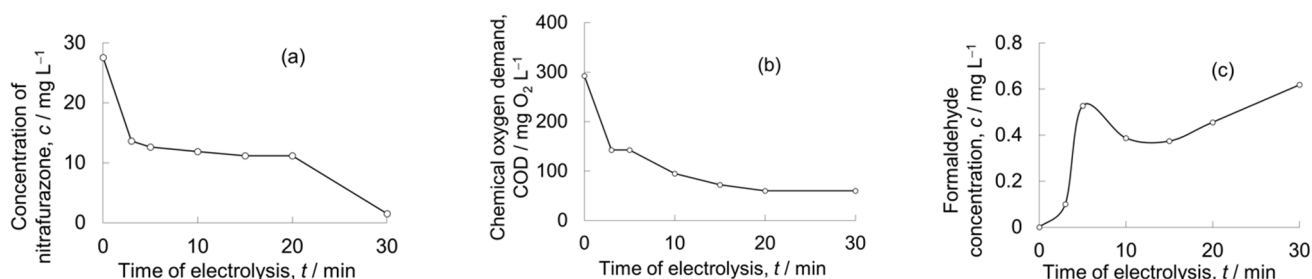


Figure 4. Nitrofurazone concentration (a), COD (b), and formaldehyde concentration (c) in the course of electrolysis using Pt/Ti anodes. See comments in the text.

The degree of nitrofurazone destruction reaches ca. 95% for 30 min of electrolysis. The values of chemical oxygen demand (COD) and total organic carbon (TOC) characterizing water quality symbatically diminish with a decrease in the concentration of nitrofurazone (Figure 4b).

The rate of nitrofurazone oxidation slows down 10–15 min after the start of electrolysis using Pt/Ti anodes (Figure 4a,b). It is rather difficult to exactly explain this effect at this stage of the study. It can be assumed that various intermediates formed during

nitrofurazone oxidation are adsorbed on the Pt surface, affecting the kinetics of oxygen evolution. As a result, the concentration of active species in the bulk of the solution decreases, causing a decrease in the nitrofurazone oxidation rate. The COD is rather high after 10–15 min of electrolysis. Later, the rate of nitrofurazone oxidation increases again (Figure 4a). This is probably due to the oxidation of inhibiting species on the electrode surface. A decrease in COD to $\sim 60 \text{ mg O}_2 \text{ L}^{-1}$ occurs after 30 min of electrochemical treatment. In addition, monocarboxylic acids are not detected in the solution after electrolysis. These results might be considered satisfactory.

However, the residual COD of about $60 \text{ mg O}_2 \text{ L}^{-1}$ after 30 min of electrolysis can be considered as being high enough. Similarly, in solutions containing 13.3 mg L^{-1} of nitrofurazone, TOC reduces from 4.85 mg L^{-1} to 3.17 mg L^{-1} in 15 min of electrochemical treatment (Table 2). Further electrolysis leads to a decrease in TOC value, though only to 2.48 mg L^{-1} .

Table 2. The TOC values after electrolysis using Pt/Ti and BDD anodes. The initial concentration of nitrofurazone is 13.3 mg L^{-1} .

Time of Electrolysis, min	TOC, mg L^{-1}	
	Pt/Ti	BDD
0	4.85	4.85
15	3.17	1.87
30	2.48	0.85

Therefore, the mineralization of nitrofurazone is not quite complete after electrochemical treatment using Pt/Ti anodes. In addition, formaldehyde is formed during electrochemical treatment (Figure 4c). This result can be considered as unfavorable due to the high toxicity of formaldehyde.

A more complete destruction of nitrofurazone after electrochemical treatment is highly desirable. This issue can be solved using the anode with a higher positive electrode potential during electrolysis. A more positive value of electrode potential promotes the formation of highly active oxygen- and chlorine-containing species, which will then destroy organic pollutants molecules. Boron-doped diamond (BDD) is an appropriate electrode material for this purpose since its oxygen evolution potential is 2.06 V ($j = 0.1 \text{ A cm}^{-2}$). This value is 210 mV more positive than that of the Pt/Ti anode (1.85 V , Figure 5).

The difference in electrode potentials at which oxygen evolution occurs on Pt/Ti and BDD anodes is due to the different mechanisms of this reaction in catalytic and non-catalytic electrodes. The evolution of oxygen on platinum proceeds through various oxygen-containing species ($\text{Pt-OH}_{\text{ads}}$ and others) adsorbed on the electrode surface. In contrast, outer sphere electron transfer takes place in the case of the BDD anode. However, as voltammetric experiments have shown, nitrofurazone does not participate in electrochemical reactions in the anodic potential region. The oxidation of nitrofurazone molecules is due to its interaction with active oxygen- and chlorine-containing species accumulated in the solution in the vicinity of the anode. The difference in both the concentration and chemical nature of these species should lead to different routes of nitrofurazone oxidation. It is highly likely that the difference in oxidation rates is explained this way.

Experiments on the electrochemical oxidation of nitrofurazone have shown that the efficiency of the BDD anode is much higher compared to the Pt/Ti anode. The concentration of nitrofurazone dropped to zero in the first half an hour of electrolysis; therefore, the degree of its destruction was about 100% (Figure 6a). This conclusion was confirmed by the residual COD ($18.0 \text{ mg O}_2 \text{ L}^{-1}$) and TOC ($<1 \text{ mg L}^{-1}$) values (Tables 2 and 3).

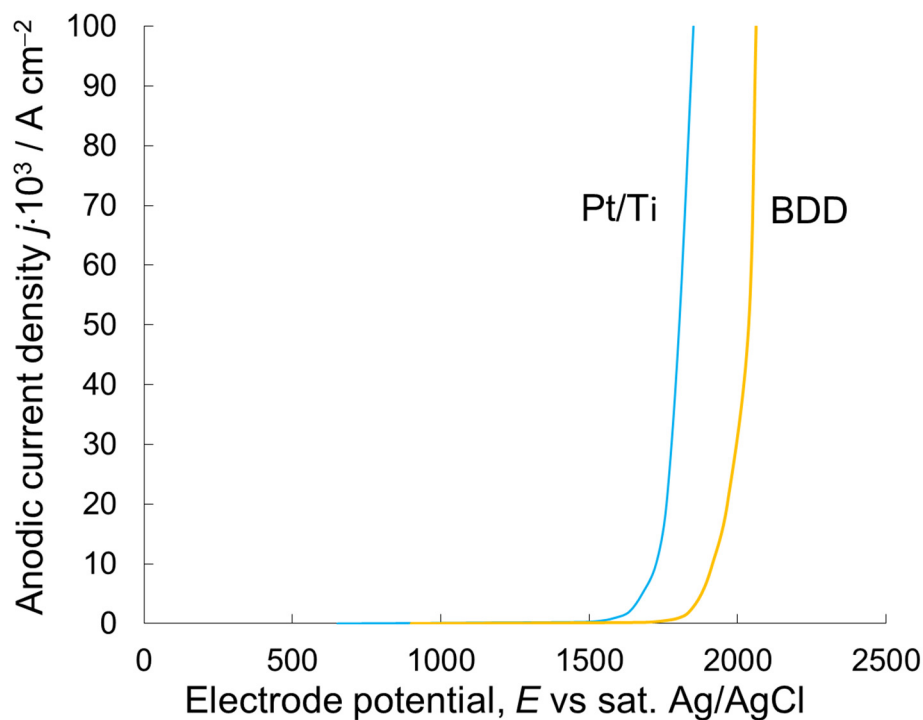


Figure 5. Potentiodynamic ($v = 1 \text{ mV s}^{-1}$) oxygen evolution polarization curves on Pt/Ti and BDD electrodes in $0.5 \text{ M H}_2\text{SO}_4$.

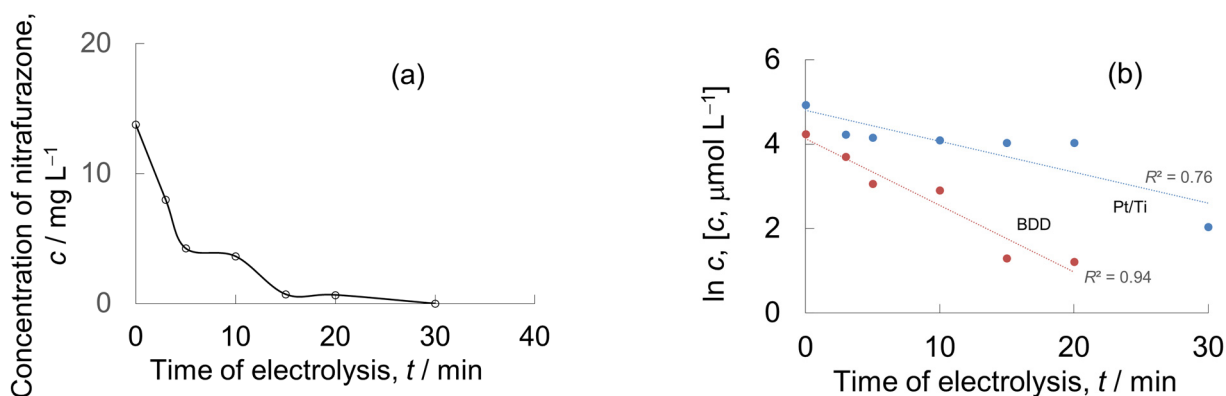


Figure 6. Changes in nitrofurazone concentration (a) in the course of electrolysis using BDD anodes and kinetic curves in first-order equation coordinates (b).

Table 3. The changes in COD and formaldehyde concentration during electrolysis with BDD anodes. The initial concentration of nitrofurazone is 13.3 mg L^{-1}

Time of Electrolysis, min	COD, $\text{mg O}_2 \text{ L}^{-1}$	Formaldehyde Concentration, mg L^{-1}
0	140	<0.1
15	45	<0.1
30	18	<0.1

It is notable that formaldehyde is not formed in the solution during electrolysis, which makes the purification process safer than in the case of using Pt/Ti anodes (Table 3). Reducing the concentration of nitrofurazone to practically zero occurred for the investigated initial concentration in the interval $10\text{--}100 \text{ mg L}^{-1}$ during 30 min of electrolysis. The optimal concentration of chloride ions should be considered in the range of $0.002\text{--}0.005 \text{ mol L}^{-1}$,

obtained after dissolving the Avexima tablet in distilled water and corresponding to its concentration in tap water. The rate of nitrofurazone mineralization slows down when the concentration of chloride ions in the solution is less than 0.002 mol L^{-1} . On the other hand, chlorine-worsening working conditions occur when the concentration of chloride ions is more than 0.005 mol L^{-1} .

The value of the redox potential (ORP) of nitrofurazone solution is equal to 0.435 V (versus standard hydrogen electrode, s.h.e, pH 2.0) before electrochemical treatment. It increases to 0.90 V (s.h.e, pH 2.0) after 30 min of electrolysis. The highly positive value of ORP indicates that the solution is well oxidized.

It should be noted that, as shown by the ICP-MS analysis of solutions after electrolysis, no degradation of electrode materials ($c(\text{Pt}) < 0.1 \text{ ppb}$, $c(\text{Ti}) < 0.5 \text{ ppb}$) was detected.

The kinetics of nitrofurazone electrooxidation using the BDD anode can be described by the first-order equation ($R^2 = 0.94$, Figure 6b). The rate constant is determined to be 0.16 min^{-1} for BDD. The data for the Pt/Ti anode do not linearize well in the coordinates of the first-order equation ($R^2 = 0.76$). Apparently, this is due to the complicated kinetics of nitrofurazone oxidation during electrolysis using this anode. Nevertheless, the rate of nitrofurazone oxidation is 2–2.5 times higher for the BDD anode. Therefore, one can conclude that BDD is a more preferable anode material both in terms of efficiency and oxidation rate. Energy consumption for the complete neutralization of nitrofurazone is estimated to be equal to $70 \text{ W}\cdot\text{h mg}^{-1}$ (BDD anode).

The better efficiency of the BDD anode compared to the Pt/Ti anode is due to the different mechanisms of oxygen evolution on them (see above). High positive electrode potentials at the BDD anode during oxygen evolution promote the formation of highly active oxygen-containing species in the volume of the treated solution. This results in the effective destruction of organic molecules.

The removal rate of nitrofurazone by electrolysis was higher compared to a water-splitting bio-photoelectrochemical cell, where about 80% of NFZ removal was achieved within 10 h of treatment [43]. An enhanced coupling photocatalysis and biodegradation method for nitrofurazone removal was proposed in [48]. In a cited article, the concentration of nitrofurazone decreased from 5 to 1 mg L^{-1} in 30 min of treatment; i.e., 80% removal of the pollutant was achieved. From this point of view, the results obtained for electrolysis with the BDD anode can be considered promising.

3.3. Identification of Products

The identification of metabolites of organic pollutants oxidation is necessary as they may be potentially hazardous. In the present study, this was carried out using Liquid Chromatography Tandem Mass Spectrometry (LC-MS-MS). Mass spectra were recorded in both positive and negative ions. As shown by mass spectrometry experiments, the nature and composition of intermediates formed at Pt/Ti and BDD anodes in the course of nitrofurazone oxidation are practically the same. The difference between these two anodes lies in the rate of accumulation and the consumption of intermediates.

Since nitrofurazone is an electron acceptor, the spectrum of nitrofurazone was observed in negative ions at a retention time of 0.3–0.5 min (Figure 7a,b).

The line at $m/z = 198$ corresponds to the ions formed upon ionization of a nitrofurazone molecule. In addition, associates with higher molecular weight are present in the mass spectra. Lines at $m/z 269$ – 272 can be assigned to ions formed upon the ionization of associates of nitrofurazone molecules with semicarbazide. It is known that semicarbazide is accumulated in the solutions of nitrofurazone as a product of its spontaneous decomposition [49]. Associates between nitrofurazone and semicarbazide molecules are formed due to hydrogen bonds between nitro and amino groups. The peaks with long retention times (5.2 min, 5.6 min, 8.6 min) seem to be associated with more complex associates, since they correspond to large m/z values in the mass spectrum.

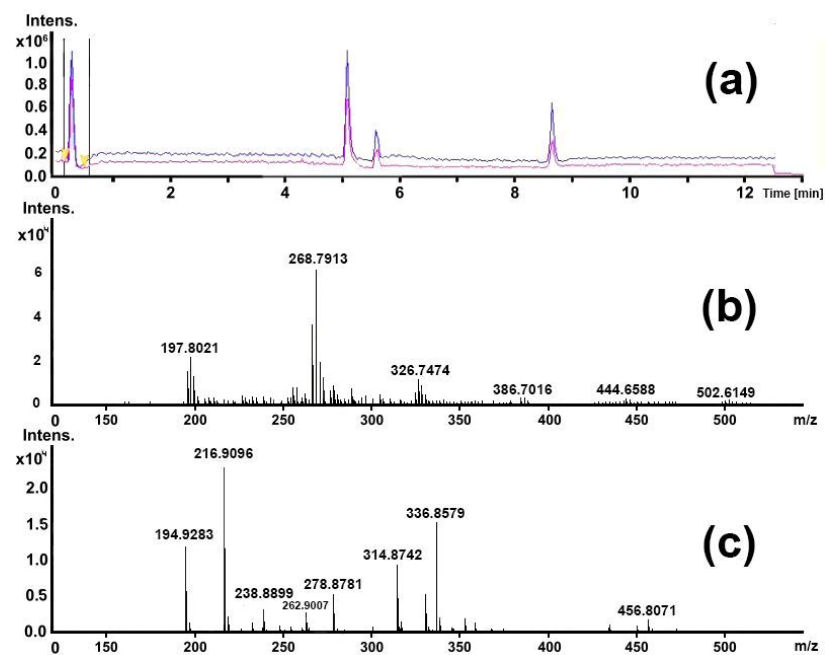


Figure 7. Chromatogram (a) and mass spectrum ($t_R = 0.3\text{--}0.5$ min) (b) in the initial solution of nitrofurazone in negative ions. The figure (c) presents the mass spectrum ($t_R = 0.3\text{--}0.5$ min) after electrochemical treatment for 30 min, BDD anode.

Lines of nitrofurazone disappeared in the mass spectrum after 30 min of electrolysis using BDD anodes (Figure 7c), which corresponds to the results of its concentration determination. The mass spectrum of the solution after electrolysis only contained residual lines of low intensity.

The nature of the intermediates formed during electrochemical treatment is better seen in the mass spectra recorded in positive ions.

The peak at $t_R = 3.9$ min present in the chromatogram was recorded in positive ions already in the initial solution of nitrofurazone (Figure 8). Its intensity increased during the first minutes of electrochemical treatment, reaching a maximum after ca. 5 min (Pt/Ti anode) and after ca. 2 min (BDD anode) after the start of electrolysis. After that, the intensity of this peak decreased and finally became negligible after 30 min of current passing.

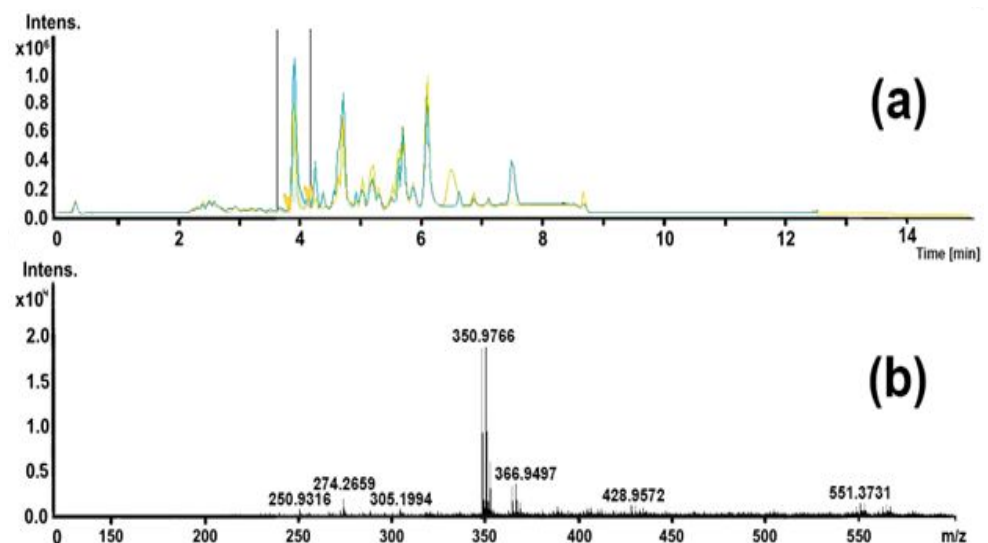


Figure 8. Chromatogram and mass spectrum ($t_R = 3.9\text{--}4.0$ min) (a,b) after 5 min of electrochemical treatment (BDD anode) in positive ions.

The ion with $m/z = 349$ dominates in the mass spectrum of the peak with $t_R = 3.9\text{--}4.0$ min; there are also ions with $m/z = 351$ and 353 . A difference in m/z value by two units indicates the presence of chlorine atoms in the molecule. The mass of the ion corresponds to the protonated form of 5-nitro-2-furaldehyde azine $[M-H]^+$ with two chlorine atoms. The structure of the discussed molecule and the pathway of its formation can be represented as follows (Figure 9):

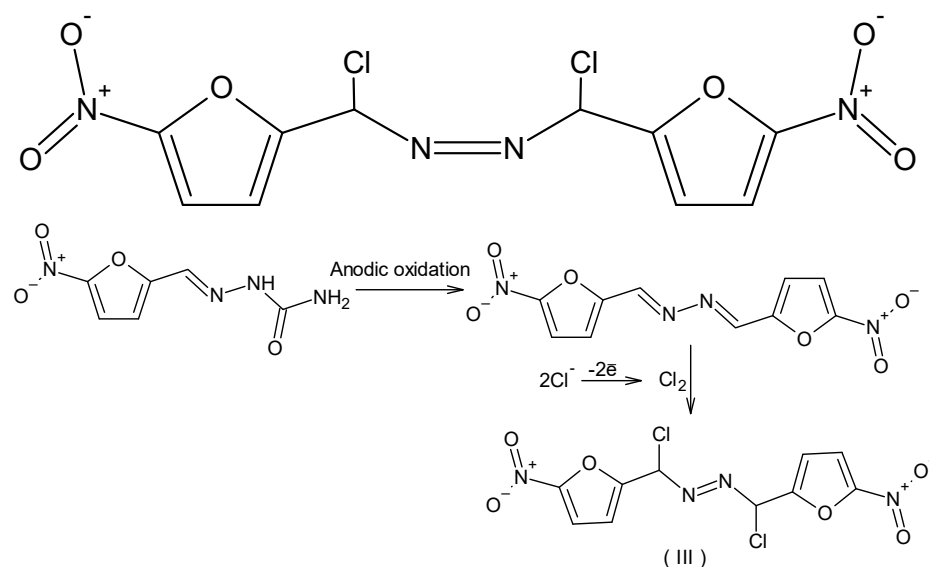


Figure 9. Chemical formula of the product of the addition of chlorine to the azine structure and the route of its formation. See comments in the text.

According to [50], 5-nitro-2-furaldehyde azine is formed upon the chlorination of aqueous solutions of nitrofurazone. The initial decoloration of nitrofurazone solution is probably due to the destruction of the system of conjugated π -bonds in its molecule. The chlorination of azines can occur by the type 1–4 addition in the azine fragment [51]. The mass spectrum also contains ions with $m/z = 365$, 367 , and 369 , which differs from the previous three by 16. It is possible that this is the product of the addition of water and the elimination of two hydrogen atoms.

The discussed intermediates accumulate in the first minutes of electrochemical treatment; however, they are destroyed by further electrolysis.

The chromatogram of the solution after 5 min of electrooxidation (Figure 8) also contains peaks ($t_R = 4.8, 5.7, 6.1$ min) corresponding to other intermediates formed during nitrofurazone electrooxidation. There are no lines different by 2 units of m/z in their mass spectra; therefore, their molecules do not contain chlorine atoms. The proposed structures of oxidation products are given in Table 4.

Oxidative polycondensation reactions are responsible for the formation of oxygen-containing intermediates of nitrofurazone. One of the possible reaction paths is given in Figure 10.

The potential toxicity of the resulting nitrofurazone oxidation intermediates was previously not known. It seems that it is advisable to apply an approach based on the use of neural networks and that published in [52] in order to evaluate it. Nevertheless, it is very important that these intermediates undergo further oxidation during electrolysis with BDD anodes, which leads to the complete mineralization of organic pollutants.

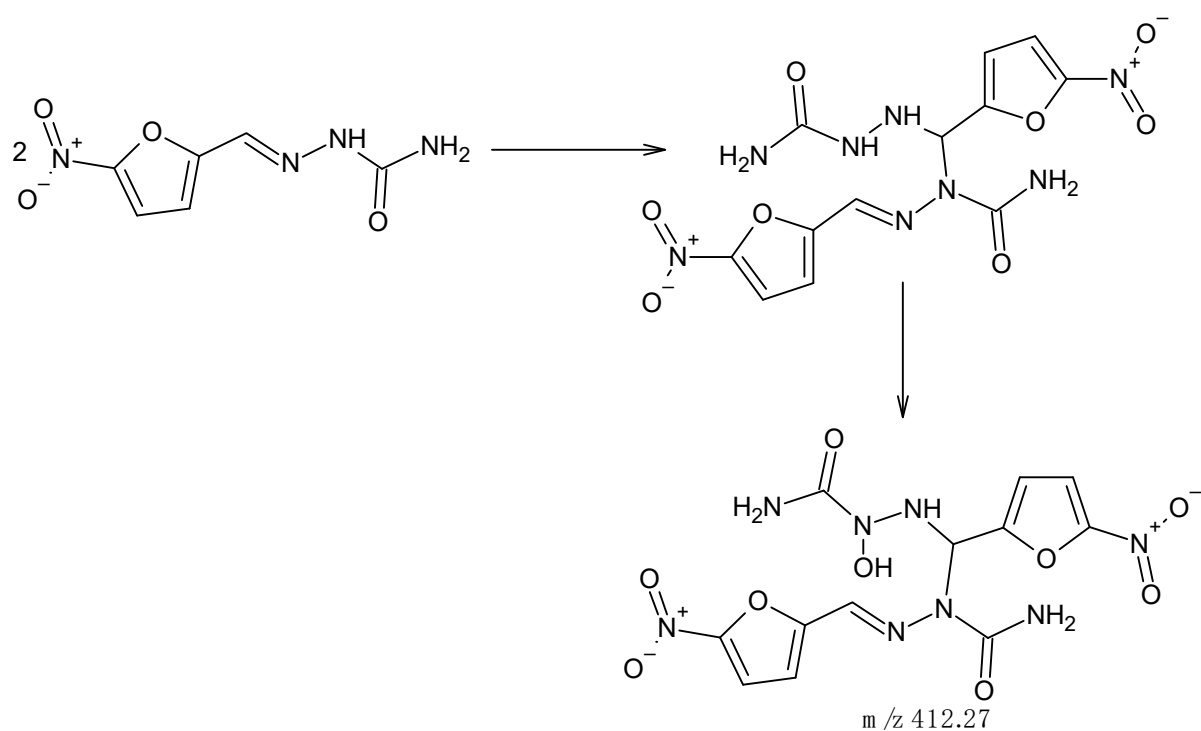


Figure 10. One of the possible reaction paths of nitrofurazone oxidative polycondensation.

Table 4. The proposed products of nitrofurazone oxidation (BDD anode, 5 min).

Retention Time, t_R , min	Dominant Peak, m/z	Proposed Structure
3.9	351, 353	
4.8	265	
5.7	413	

Table 4. Cont.

Retention Time, t_R , min	Dominant Peak, m/z	Proposed Structure
6.1	569	

4. Conclusions

The electrochemical oxidative degradation of nitrofurazone in aqueous solutions in the presence of chloride ions was performed. Solutions under the electrochemical treatment contained 10–100 mg L⁻¹ of nitrofurazone. Electrolysis was carried out under galvanostatic conditions at an anodic current density of 0.1 A cm⁻² and a volume current density of 1.33 A L⁻¹ for 30 min.

Since nitrofurazone reduces in the cathodic region of potentials, cathodic and anodic compartments of the electrochemical cell should be separated in order to exclude the cost of electricity on the reduction of nitrofurazone at the cathode and the subsequent oxidation of formed products at the anode. The separation of cathode and anode compartments also prevents the accumulation of nitrofurazone reduction products of various chemical natures in the solution under electrochemical treatment.

In principle, the electrochemical destruction of nitrofurazone is possible on both Pt/Ti and BDD anodes; however, the process is more efficient and safe when using BDD anodes. The preference for using BDD anodes is due to their higher electrode potential during electrolysis, which leads to a higher rate of active species generation.

The addition of the products of chlorine to 5-nitro-2-furaldehyde azine was formed in the solution under electrochemical treatment in the first minutes (0–15 min) of electrolysis. Almost complete mineralization of organic pollutants occurred after ca. 30 min of electrolysis using BDD anodes. Therefore, electrochemical treatment for 30 min can be recommended for the mineralization of nitrofurazone.

Supplementary Materials: The following supporting information can be downloaded at: <https://www.mdpi.com/article/10.3390/w15193370/s1>.

Author Contributions: V.V.K. Conceptualization, Methodology, Writing, N.A.I.—intermediate analytical control, selection of experimental conditions, Data Processing, E.N.K.—literature review, writing, experiment, A.V.P.—analytical control, description of the mechanism of destruction, Y.O.M.—interpretation of the results obtained, E.A.F.—analytical control of oxidation products. Writing, Y.M.A.—experiment, Data Processing. All authors have read and agreed to the published version of the manuscript.

Funding: This work was supported by the Russian Science Foundation grant no. 23-23-00067.

Institutional Review Board Statement: Not applicable.

Informed Consent Statement: Not applicable.

Data Availability Statement: The data can be found within the manuscript.

Acknowledgments: This work was supported by the Russian Science Foundation grant no. 23-23-00067.

Conflicts of Interest: The authors declare that they have no known competing financial interest or personal relationship that could have appeared to influence the work reported in this paper.

References

1. Wang, Q.; Wang, P.; Yang, Q. Occurrence and diversity of antibiotic resistance in untreated hospital wastewater. *Sci. Total Environ.* **2018**, *621*, 990–999. [[CrossRef](#)] [[PubMed](#)]
2. Aali, R.; Nikaeen, M.; Khanahmad, H.; Hassanzadeh, A. Monitoring and comparison of antibiotic resistant bacteria and their resistance genes in municipal and hospital wastewaters. *Int. J. Prev. Med.* **2014**, *5*, 887–894. [[PubMed](#)]
3. Adator, E.H.; Narvaez-Bravo, C.; Zaheer, R.; Cook, S.R.; Tymensen, L.; Hannon, S.J.; Booker, C.W.; Church, D.; Read, R.R.; McAllister, T.A. A one health comparative assessment of antimicrobial resistance in generic and *Escherichia coli* from beef production, sewage and clinical settings. *Microorganisms* **2020**, *8*, 885. [[CrossRef](#)] [[PubMed](#)]
4. Aubertreau, E.; Stalder, T.; Mondamert, L.; Ploy, M.-C.; Dagot, C.; Labanowski, J. Impact of wastewater treatment plant discharge on the contamination of river biofilms by pharmaceuticals and antibiotic resistance. *Sci. Total Environ.* **2017**, *579*, 1387–1398. [[CrossRef](#)]
5. Thomas, K.V.; Langford, K.H. Point Sources of Human Pharmaceuticals into the Aquatic Environment. In *Green and Sustainable Pharmacy*; Kümmerer, K., Hempel, M., Eds.; Springer: Berlin/Heidelberg, Germany, 2010; pp. 211–223.
6. Kotwani, A.; Joshi, J.; Kaloni, D. Pharmaceutical effluent: A critical link in the interconnected ecosystem promoting antimicrobial resistance. *Environ. Sci. Pollut. Res. Int.* **2021**, *28*, 32111–32124. [[CrossRef](#)] [[PubMed](#)]
7. Kabanov, M.A.; Ivantsova, N.A.; Kuzin, E.N.; Murzina, E.D.; Korobov, A.Y. Evaluation of the influence of drug complex formation on the efficiency of water conditioning with reagents for tetracycline. *Pharm. Chem. J.* **2022**, *55*, 1245–1249. [[CrossRef](#)]
8. Li, C.; Xu, Y.; Song, W. Pollution Characteristics and Risk Assessment of Typical Antibiotics and Persistent Organic Pollutants in Reservoir Water Sources. *Water* **2023**, *15*, 259. [[CrossRef](#)]
9. Wang, P.; He, Y.L.; Huang, C.H. Reactions of tetracycline antibiotics with chlorine dioxide and free chlorine. *Water Res.* **2011**, *45*, 1838–1846. [[CrossRef](#)]
10. Gu, C.; Karthikeyan, K.G. Interaction of tetracycline with aluminum and iron hydrous oxides. *J. Environ. Sci. Technol.* **2005**, *39*, 2660–2667. [[CrossRef](#)]
11. Ng, K.; Alygizakis, N.A.; Thomaidis, N.S.; Slobodnik, J. Wide-Scope Target and Suspect Screening of Antibiotics in Effluent Wastewater from Wastewater Treatment Plants in Europe. *Antibiotics* **2023**, *12*, 100. [[CrossRef](#)]
12. Pereira, A.; Silva, L.J.G.; Laranjeiro, C.S.M.; Meisel, L.M.; Lino, C.M.; Pena, A. Human pharmaceuticals in Portuguese rivers: The impact of water scarcity in the environmental risk. *Sci. Total Environ.* **2017**, *609*, 1182–1191. [[CrossRef](#)] [[PubMed](#)]
13. Kim, H.-Y.; Lee, I.-S.; Oh, J.-E. Human and veterinary pharmaceuticals in the marine environment including fish farms in Korea. *Sci. Total Environ.* **2017**, *579*, 940–949. [[CrossRef](#)] [[PubMed](#)]
14. Gevao, B.; Uddin, S.; Dupont, S. Baseline concentrations of pharmaceuticals in Kuwait’s coastal marine environment. *Mar. Pollut. Bull.* **2021**, *173*, 113040. [[CrossRef](#)]
15. Younes, H.A.; Mahmoud, H.M.; Abdelrahman, M.M.; Nassar, H.F. Seasonal occurrence, removal efficiency and associated ecological risk assessment of three antibiotics in a municipal wastewater treatment plant in Egypt. *Environ. Nanotechnol. Monit. Manag.* **2019**, *12*, 100239. [[CrossRef](#)]
16. Qiao, M.; Ying, G.-G.; Singer, A.C.; Zhu, Y.-G. Review of antibiotic resistance in China and its environment. *Environ. Int.* **2018**, *110*, 160–172. [[CrossRef](#)]
17. Pan, M.; Chu, L.M. Occurrence of antibiotics and antibiotic resistance genes in soils from wastewater irrigation areas in the Pearl River Delta region, southern China. *Sci. Total Environ.* **2018**, *624*, 145–152. [[CrossRef](#)]
18. Tiwari, A.; Kurittu, P.; Al-Mustapha, A.I.; Heljanko, V.; Johansson, V.; Thakali, O.; Mishra, S.K.; Lehto, K.M.; Lipponen, A.; Oikarinen, S.; et al. WastPan Study Group; A. Heikinheimo, Wastewater surveillance of antibiotic-resistant bacterial pathogens: A systematic review. *Front. Microbiol.* **2022**, *13*, 977106. [[CrossRef](#)]
19. Desai, M.; Njoku, A.; Nimo-Sefah, L. Comparing Environmental Policies to Reduce Pharmaceutical Pollution and Address Disparities. *Int. J. Environ. Res. Public Health* **2022**, *19*, 8292. [[CrossRef](#)]
20. Kusturica, M.P.; Jevtic, M.; Ristovski, J.T. Minimizing the environmental impact of unused pharmaceuticals: Review focused on prevention. *Front. Environ. Sci.* **2022**, *10*, 1077974. [[CrossRef](#)]
21. de Ilurdoz, M.S.; Sathwani, J.J.; Reboso, J.V. Antibiotic removal processes from water & wastewater for the protection of the aquatic environment—A review. *J. Water Process Eng.* **2022**, *45*, 102474.
22. Wang, J.; Wang, S. Removal of pharmaceuticals and personal care products (PPCPs) from wastewater: A review. *J. Environ. Manag.* **2016**, *182*, 620–640. [[CrossRef](#)] [[PubMed](#)]
23. Zhang, D.; Gersberg, R.M.; WJ, N.; SK, T. Removal of pharmaceuticals and personal care products in aquatic plant-based systems: A review. *Environ. Pollut.* **2014**, *184*, 620–639. [[CrossRef](#)] [[PubMed](#)]
24. Loganathan, P.; Vigneswaran, S.; Kandasamy, J.; Cuprys, A.K.; Maletskyi, Z.; Ratnaweera, H. Treatment Trends and Combined Methods in Removing Pharmaceuticals and Personal Care Products from Wastewater—A review. *Membranes* **2023**, *13*, 158. [[CrossRef](#)] [[PubMed](#)]

25. Kanakaraju, D.; Glass, B.D.; Oelgemöller, M. Advanced oxidation process-mediated removal of pharmaceuticals from water: A review. *J. Environ. Manag.* **2018**, *219*, 189–207. [[CrossRef](#)]
26. Thiruvénkatachari, R.; Vigneswaran, S.; Moon, I.S. A review on UV/TiO₂ photocatalytic oxidation process. *Korean J. Chem. Eng.* **2008**, *25*, 64–72. [[CrossRef](#)]
27. Sharma, S.; Ruparelia, J.P.; Patel, M.L. A General Review on Advanced Oxidation Processes for Waste Water Treatment. In Proceedings of the Nirma University International Conference, Ahmedabad, India, 8–10 December 2011.
28. Jiao, J.; Li, Y.; Song, Q.; Wang, L.; Luo, T.; Gao, C.; Liu, L.; Yang, S. Removal of Pharmaceuticals and Personal Care Products (PPCPs) by Free Radicals in Advanced Oxidation Processes. *Materials* **2022**, *15*, 8152. [[CrossRef](#)]
29. Emzhina, V.V.; Kuzin, E.N.; Babusenko, E.S.; Krutchinina, N.E. Photodegradation of tetracycline in presence of H₂O₂ and metal oxide based catalysts. *J. Water Process Eng.* **2021**, *39*, 101696. [[CrossRef](#)]
30. Mylapilli, S.V.P.; Reddy, S.N. Sub and supercritical water oxidation of pharmaceutical wastewater. *J. Environ. Chem. Eng.* **2019**, *7*, 103165. [[CrossRef](#)]
31. Johnston, J.B.; Hannah, R.E.; Cunningham, V.L.; Daggy, B.P.; Sturm, F.J.; Kelly, R.M. Destruction of Pharmaceutical and Biopharmaceutical Wastes by the Modar Supercritical Water Oxidation Process. *Nat. Biotechnol.* **1988**, *6*, 1423–1427. [[CrossRef](#)]
32. Trellu, C.; Chaplin, B.P.; Coetsier, C.; Esmilaire, R.; Cerneaux, S.; Causserand, C.; Cretin, M. Electro-oxidation of organic pollutants by reactive electrochemical membranes. *Chemosphere* **2018**, *208*, 159–175. [[CrossRef](#)]
33. Lan, Y.; Coetsier, C.; Causserand, C.; Serrano, K. An experimental and modelling study of the electrochemical oxidation of pharmaceuticals using a boron-doped diamond anode. *Chem. Eng. J.* **2018**, *333*, 486–494. [[CrossRef](#)]
34. Yang, Y.; Ramos, N.C.; Clark, J.A.; Hillhouse, H.W. Electrochemical oxidation of pharmaceuticals in synthetic fresh human urine: Using selective radical quenchers to reveal the dominant degradation pathways and the scavenging effects of individual urine constituents. *Water Res.* **2022**, *221*, 118722. [[CrossRef](#)]
35. da Silva, S.W.; Welter, J.B.; Albornoz, L.L.; Heberle, A.N.; Ferreira, J.Z.; Bernardes, A.M. Advanced Electrochemical Oxidation Processes in the Treatment of Pharmaceutical Containing Water and Wastewater: A Review. *Curr. Pollut. Rep.* **2021**, *7*, 146–159. [[CrossRef](#)]
36. Karaoğlu, G.; Öztürk, D.; Akyol, A.; Kara, S. PCT degradation with electrooxidation (EOx) and ultrasound (US) hybrid process using different type electrodes: BDD, Ti/PbO₂ and Ti/Pt. *Sep. Purif. Technol.* **2023**, *311*, 123313. [[CrossRef](#)]
37. Köktaş, Y.; Gökkuş, Ö.; Kariper, İ.A.; Othmani, A. Tetracycline removal from aqueous solution by electrooxidation using ruthenium-coated graphite anode. *Chemosphere* **2023**, *315*, 137758. [[CrossRef](#)] [[PubMed](#)]
38. Kuznetsov, V.V.; Kapustin, E.S.; Pirogov, A.V.; Kurdin, K.A.; Filatova, E.A.; Kolesnikov, V.A. An effective electrochemical destruction of non-ionic surfactants on bismuth-modified lead dioxide anodes for wastewater pretreatment. *Solid. State Electrochem.* **2020**, *24*, 173–183. [[CrossRef](#)]
39. Fu, R.; Zhang, P.-S.; Jiang, Y.-X.; Sun, L.; Sun, X.-H. Wastewater treatment by anodic oxidation in electrochemical advanced oxidation process: Advance in mechanism, direct and indirect oxidation detection methods. *Chemosphere* **2023**, *311*, 136993. [[CrossRef](#)]
40. Bellver-Domingo, A.; Fuentes, R.; Hernández-Sancho, F. Shadow prices of emerging pollutants in wastewater treatment plants: Quantification of environmental externalities. *J. Environ. Manag.* **2017**, *203*, 439–447. [[CrossRef](#)]
41. Symes, D.; Al-Duri, B.; Bujalski, W.; Dhir, A. Cost-effective design of the alkaline electrolyser for enhanced electrochemical performance and reduced electrode degradation. *Int. J. Low-Carbon Technol.* **2015**, *10*, 452–459. [[CrossRef](#)]
42. Aviezer, Y.; Lahav, O. Removal of contaminants of emerging concern from secondary-effluent reverse osmosis retentates by continuous supercritical water oxidation parametric study and conceptual design. *J. Hazard. Mater.* **2022**, *437*, 129379. [[CrossRef](#)]
43. Hou, Y.; Yuan, G.; Wang, S.; Yu, Z.; Qin, S.; Tu, L.; Yan, Y.; Chen, X.; Zhu, H.; Tang, Y. Nitrofurazone degradation in the self-biased bio-photoelectrochemical system: g-C₃N₄/CdS photocathode characterization, degradation performance, mechanism and pathways. *J. Hazard. Mater.* **2020**, *384*, 121438. [[CrossRef](#)] [[PubMed](#)]
44. Shmychkova, O.; Zahorulko, S.; Girenko, D.; Luk, T.; Dmitrikova, L.; Velichenko, A. Material Selection and Optimization of Conditions for Electrooxidation of Nitrofurazone: A Comparative Study of Tin and Lead Dioxides. *J. Electrochem. Soc.* **2021**, *168*, 086507. [[CrossRef](#)]
45. Brito, C.L.; Ferreira, E.I.; La-Scalea, M.A. Application of multi-walled carbon nanotubes functionalized with hemin to evaluate the electrochemical behavior of nitrofurazone in aqueous media. *Electrochim. Acta* **2023**, *459*, 142486. [[CrossRef](#)]
46. Rahi, A.; Sattarahmady, N.; Vais, R.D.; Heli, H. Sono-electrodeposition of gold nanorods at a gold surface—Application for electrocatalytic reduction and determination of nitrofurazone. *Sens. Actuators B* **2015**, *210*, 96–102. [[CrossRef](#)]
47. Jiang, Y.; Zhao, H.; Liang, J.; Yue, L.; Li, T.; Luo, Y.; Liu, Q.; Lu, S.; Asiri, A.M.; Gong, Z.; et al. Anodic oxidation for the degradation of organic pollutants: Anode materials, operating conditions and mechanisms. A mini review. *Electrochem. Commun.* **2021**, *123*, 106912. [[CrossRef](#)]
48. Smulek, W.; Bielan, Z.; Zgoła-Grzeškowiak, A.; Zielińska-Jurek, A.; Kaczorek, E. Nitrofurazone Removal from Water Enhanced by Coupling Photocatalysis and Biodegradation. *Int. J. Mol. Sci.* **2021**, *22*, 2186. [[CrossRef](#)]
49. Li, G.; Tang, C.; Wang, Y.; Yang, J.; Wu, H.; Chen, G.; Kong, X.; Kong, W.; Liu, S.; You, J. A Rapid and Sensitive Method for Semicarbazide Screening in Foodstuffs by HPLC with Fluorescence Detection. *Food Anal. Methods* **2015**, *8*, 1804–1811. [[CrossRef](#)]
50. Nakamura, H.; Kawakami, T.; Niino, T.; Takahashi, Y.; Onodera, S. Chemical fate and changes in mutagenic activity of antibiotics nitrofurazone and furazolidone during aqueous chlorination. *J. Toxicol. Sci.* **2008**, *33*, 621–629. [[CrossRef](#)]

51. Al-Masoudi, N.A.; Al-Soud, Y.A.; Ali, I.A.I. Synthesis of 1,2,4-triazole C-nucleosides from hydrazonyl chlorides and nitriles. *Nucleosides Nucleotides Nucleic Acids* **2007**, *26*, 37–43. [[CrossRef](#)]
52. Cremer, J.; Sandonas, L.M.; Tkatchenko, A.; Clevert, D.-A.; Fabritiis, C.D. Equivariant Graph Neural Networks for Toxicity Prediction. *Chem. Res. Toxicol.* **2023**. [[CrossRef](#)]

Disclaimer/Publisher’s Note: The statements, opinions and data contained in all publications are solely those of the individual author(s) and contributor(s) and not of MDPI and/or the editor(s). MDPI and/or the editor(s) disclaim responsibility for any injury to people or property resulting from any ideas, methods, instructions or products referred to in the content.